Int. J. Solids Structures Vol. 18, No. 9, pp. 737–762, 1982
Printed in Great Britain.

0020–7683/82/090737–26$03.00/0
Pergamon Press Ltd.

IMPROVED FINITE ELEMENT MODELS FOR THE LARGE DISPLACEMENT BENDING AND POST BUCKLING ANALYSIS OF THIN PLATES

D. J. ALLMAN
Royal Aircraft Establishment, Farnborough, England

(*Received* 21 *July* 1981; *in revised form* 29 *December* 1981)

Abstract—Triangular finite element models are presented for the large displacement bending and post-buckling analysis of thin plates. The formulation is based upon a general variational theory which offers a wide scope for the selection of valid finite element trial functions. This makes it feasible to model the particular physical actions crucial to the successful calculation of large displacement behaviour. In this paper it is demonstrated by numerical examples that a notable improvement in performance is achieved, without a significant increase in computational effort, when simple inextensional bending deformations are included explicitly in the finite element trial functions.

NOTATION

a_i	six rigid body movements of a plate
a_0	amplitude of eigenvector in eqn (5–10)
A	area of a plate
B, C	matrices defined in eqns (3–35)
D	flexural rigidity of a plate, defined in eqn (6–2)
e_{11}, e_{22}, e_{12}	constant membrane strains
E	Young's modulus
$E_x, E_y, E_z, \bar{E}_z$	components of the special column vectors $\mathbf{E}$ and $\bar{\mathbf{E}}$
f	quartic polynomial, defined in eqn (5-2)
F	nonlinear energy function, defined in eqn (5-4)
g_α, g_β	column vectors of generalized displacements for bending and stretching actions, defined in eqns (3-30) and (3-34)
G_α, G_β	column vectors of generalized forces for bending and stretching actions, defined in eqns (3-28) and (3-32)
h	thickness of a plate
h_{ijkl}	coefficients of quartic polynomial, defined in eqn (5-2)
$H_{\alpha\alpha}, H_{\beta\beta}$	matrices defined in eqns (4-1)
I_α, I_β	defined in eqns (3-24)
k_{11}, k_{22}, k_{12}	constant curvatures and twist
K_n	Kirchhoff shear force
K^0_{ij}, K^1_{ij}	elements of linear elastic and geometric stiffness matrices
K^2_{ij}	elements of matrix defined in eqn (5-8)
l_{12}	length of side $1 \rightarrow 2$ of a finite element
L_α	column vector defined in eqn (4-2)
M_x, M_y, M_{xy}	Cartesian components of bending and twisting moments
M_n, M_{nt}	normal bending moment and twisting moment
$M_{\beta\beta}$	matrix defined in eqn $(4\text{-}12)_1$
n, t	normal and tangential coordinates at a plate edge
N_x, N_y, N_{xy}	Cartesian components of stress resultants
N_n, N_{nt}	normal and tangential components of stress resultants
$N_{\beta\beta}$	matrix defined in eqn (4-2)
N_T	total number of bending degrees-of-freedom x_i
p^*_z	prescribed normal pressure on a plate
P^*	column vector defined in eqn (4-3)
P_α	column vector defined in eqn (3-8)
q_α, q_β	column vectors containing the connection quantities for bending and stretching actions, defined in eqns (3-7)
R_N	Kirchhoff force resultant at a corner point N
R_α	column vector defined in eqn $(4\text{-}12)_2$
s	coordinate measured along a plate edge or around a finite element boundary
S, T	matrices defined in eqns (4-5)
U, V, W	components of displacement in the x, y, z directions
U_n, U_t	normal and tangential components of U, V displacements
V_n	total shear force, defined in eqn (2-9)
W_n	normal displacement at a corner point N
x, y, z	rectangular Cartesian coordinates
x_i	bending degrees-of-freedom for a finite element mesh
x^0_i	starting values of x_i for post-buckling analysis
X^*, Y^*	prescribed body forces in the plane of a plate

Greek symbols

- α, β column vectors containing the coefficients of the assumed bending and twisting moments and the assumed stress resultants, defined in eqns (3-36)
- γ_{12} angle between the exterior normal and the x direction on the side $1 \rightarrow 2$ of a finite element
- Γ defined in eqn (4-12)
- Δ area of a triangular element
- $\epsilon_x, \epsilon_y, \gamma_{xy}$ Cartesian components of strain
- η eigenvector corresponding to initial buckling mode
- θ_n normal rotation $(= -(\partial W/\partial n))$
- κ principal curvature, defined in eqns (3-5)
- $\kappa_x, \kappa_y, \kappa_{xy}$ Cartesian components of curvature and twist
- Λ defined in eqn (4-2)
- μ intensity of applied membrane loading
- ν Poisson's ratio
- ξ_1, ξ_2, ξ_3 triangular coordinates, defined in eqn (3-10)
- Π_{FE} generalized complementary energy functional for a complete plate
- π_e generalized complementary energy functional for a single finite element
- ρ constant coefficient in iterative method
- ϕ angle between generators and x direction
- Ω potential function for prescribed body forces X^*, Y^*

Script symbols

- $\mathscr{B}$ matrix defined in eqn (2-5)
- $\mathscr{C}$ total boundary of a finite element
- $\mathscr{C}_K, \mathscr{C}_T$ parts of a plate edge or finite element boundary subjected to kinematic or traction conditions
- $\mathscr{F}, \mathscr{H}$ matrices containing the elastic and geometric properties of a plate for bending and stretching action respectively

Subscripts

- α, β refers to bending and stretching action respectively
- e refers to the eth finite element
- i, j, k, l dummy suffices
- N refers to corner point of a finite element

Superscripts

- r iteration counter
- T transpose of a matrix or vector
- $*$ prescribed value or exact value
- $\sim$ variable defined as a function of s only

Special column vectors

$$\underline{\mathbf{E}} = (E_x E_y E_z)^T$$
$$\bar{\mathbf{E}} = (E_s E_y E_z)^T$$
$$\mathbf{M} = (M_x M_y M_{xy})^T$$
$$\mathbf{N} = (N_x N_y N_{xy})^T$$
$$\mathbf{p}^* = (X^* Y^* p_z^*)^T$$
$$\underline{\mathbf{R}} = (N_n N_{nt} R_N V_n M_n)^T$$
$$\bar{\mathbf{R}} = (N_n N_{nt} R_N K_n M_n)^T$$
$$\mathbf{R}^* = (N_n^* N_{nt}^* R_N^* V_n^* M_n^*)^T$$
$$\underline{\mathbf{U}} = (U V W)^T$$
$$\bar{\mathbf{U}} = (\bar{U}_n \bar{U}_t \bar{W}_N \bar{W} \bar{\theta}_n)^T$$
$$\mathbf{U}^* = (U_n^* U_t^* W_N^* W^* \theta_n^*)^T$$
$$\theta = \left(\frac{\partial W}{\partial x} \frac{\partial W}{\partial y}\right)^T$$

1. INTRODUCTION

Thin plate components are frequently employed in the construction of modern aerospace structures. Indeed, many applications of new lightweight materials such as carbon fibre reinforced plastic involve the use of rather thin laminates. Now, the bending behaviour of thin plates under normal loading shows a marked departure from the prediction of the linear theory[1, 2] for small normal displacements. Moreover, it is well-known that under plane compression or shear loadings there is often quite adequate stiffness for structural requirements long after initial buckling has occurred. The present paper is concerned with the development of finite element models for accurate analysis of the class of plate problems covered by the nonlinear theory of von Kármán[3]. The approach is therefore restricted to situations where the angles of rotation of the plate mid-surface are small compared to unity, but this is not too severe a limitation in practice because normal displacements several times larger than the plate thickness are permitted; bending with larger normal displacements than this is, in any case, unacceptable in typical aircraft structures.

The finite element models which are presented in the paper employ separate trial functions for the stress resultants, stress couples and displacements of a plate. This concept was first introduced by Pian in his "hybrid stress" formulation for plane stress analysis[4] which he later extended to the small displacement bending analysis of plates[5], rectangular elements being used in both cases. Triangular finite elements for the plate bending problem using the hybrid stress formulation are given by Allman[6]. The method is an application of a variational principle in which the stresses are constrained to satisfy the equations of equilibrium inside an element and the displacements are defined as a one-dimensional compatible distribution on the element boundary. This latter feature avoids the algebraic complications encountered in defining two-dimensional normal displacement fields with continuous first derivatives as required for valid applications of the traditional displacement method to plate bending problems.

An application of the hybrid stress method to the analysis of initial buckling of plates is given by Tabarrok and Gass[7]. Their results are obtained using rectangular elements for square plates under uniform plane loadings, but it is reported that the method is prone to matrix singularities under certain conditions. It also requires the numerical solution of a nonlinear eigenvalue problem. By contrast, an alternative finite element analysis for plate buckling, presented by Allman[8], is well behaved in all instances and presents a conventional linear eigenvalue problem for calculation of the elastic buckling loads. The formulation is not a standard hybrid stress model because only the linear part of the normal equilibrium equation is satisfied exactly inside an element. Nevertheless, the approach is rigorously based upon a variational principle for stresses and displacements. It is found to give reliable and accurate results in extensive applications with triangular elements[9]. A comparison of this type of finite element model with the standard hybrid stress model is undertaken by Boland and Pian[10] in their large deflection analysis of thin elastic arches and shells. They conclude that the two models yield essentially the same results.

The present paper develops improved finite element models for the large displacement bending and post-buckling analysis of thin plates. It is shown in Section 2 that these models are based upon a variational theory[11] for large displacement bending which includes, as special cases, the variational principles used for the finite element analysis of small displacement bending[6] and initial buckling[8] of plates. The formulation is free from restrictive subsidiary conditions on the stress and displacement variables, thus offering a wide scope for the selection of finite element trial functions to model the particular physical actions identified[12] as crucial to the successful calculation of large displacement behaviour. Indeed, it is shown in Section 3.2 that basic trial functions, which are selected to recover exactly the rigid body movements and constant states of membrane strain, can also be easily augmented to allow exact recovery of simple inextensional bending deformations. These modes of deformation are considered to have an important influence on the convergence of finite element approximations to the exact solution with successive mesh refinement. Further developments to deal with more complicated types of physical action, such as boundary layer effects, also appear to be feasible using this type of approach. Some alternative variational formulations for large deformation analysis of plates are given by Tabarrok and Dost[19].

A "basic" triangular finite element model, with simple polynomial expansions for the trial functions, is presented in Section 4.1. The relevant trial functions are given in Section 3.1 and they correspond exactly to those used previously in the finite element schemes for buckling analysis[8, 9] and large deflection analysis[10]. Accordingly, it is assumed that the membrane stress resultants are constant and the bending and twisting moments are linear. This ensures satisfaction of the homogeneous plane equilibrium equations and the linear part of the equation of normal equilibrium. The normal displacements are cubic polynomials where, to avoid difficulties concerning boundary compatibility, separate assumptions are made for the distribution inside each element and on the element boundary, as in the standard hybrid stress model. The membrane displacements are also defined separately inside an element and on the element boundary; they are linear functions. The basic finite element model has five nodal connection quantities defined at each of the element corners, *viz* the normal displacement and its two first derivatives and the two components of membrane displacement.

New finite element models which permit exact recovery of simple inextensional bending behaviour are presented in Sections 4.2 and 4.3. They are denoted in the text as an "augmented

displacements model" and an "equilibrium model for stretching" respectively. The augmented displacements model is the more efficient for numerical computation; it has nodal connection quantities located at the element corners which are identical to the basic model described above. The equilibrium model requires nodal connection quantities on the element sides, thereby increasing the number of equations involved in a numerical solution. This approach is less attractive for practical applications and no results are presented here.

A selection of numerical examples is given in Section 6 which enables a comparison to be made between the basic finite element model and the augmented displacements model. The examples cover various kinds of elastic behaviour typical of the large displacement bending and post-buckling of thin plates. It is found that there is a notable improvement in the performance of the augmented displacements model over that of the basic model which is a direct consequence of including simple inextensional bending deformations in the finite element trial functions. Yet there is no significant increase in the computational effort required for a numerical solution when this feature is incorporated in the analysis. The examples also show that the basic model has an undesirable sensitivity to some finite element mesh arrangements and its convergence characteristics are often poor; indeed, completely unacceptable results are obtained in one instance. By contrast, in all cases where the effect of refining the finite element mesh is investigated, the results from the augmented displacements model exhibit rapid and smooth convergence to the final solution. This provides a first validation of the fundamental requirements proposed [12] for accurate finite element analysis of nonlinear elastic plate bending.

2. VARIATIONAL THEORY FOR FINITE ELEMENT ANALYSIS

The finite element analysis is based upon a general variational theory[11] for the large displacement bending behaviour of thin plates. The method of solution involves finding the stationary values of a generalized complementary energy functional which employs separately assumed fields for the stress resultants, stress couples and displacements of a plate. For convenience of application, the complementary energy functional is expressed in a concise way using a matrix notation with special column vectors defined for the field variables as follows:

Functions of x *and* y	*Functions of* s
$\mathbf{U} = (UVW)^T,$	$\tilde{\mathbf{U}} = (\tilde{U}_n \tilde{U}_t \tilde{W}_N \tilde{W} \tilde{\theta}_n)^T,$
$\theta = \left(\frac{\partial W}{\partial x} \frac{\partial W}{\partial y}\right)^T,$	$\mathbf{U}^* = (U_n^* U_t^* W_N^* W^* \theta_n^*)^T,$
$\mathbf{M} = (M_x M_y M_{xy})^T,$	$\mathbf{R} = (N_n N_{nt} R_N V_n M_n)^T,$
$\mathbf{N} = (N_x N_y N_{xy})^T,$	$\tilde{\mathbf{R}} = (N_n N_{nt} R_N K_n M_n)^T,$
$\mathbf{p}^* = (X^* Y^* p_z^*)^T,$	$\mathbf{R}^* = (N_n^* N_{nt}^* R_N^* V_n^* M_n^*)^T.$ (2-1)

The rectangular Cartesian coordinates x, y, z form a right-handed set, where x and y are in the plane of the plate, and the coordinate s is measured along the edge of the plate. Variables like W in the left-hand list of eqns (2-1) are functions of the coordinates x and y, whereas variables like $\tilde{W}$ in the right-hand list are functions of the coordinate s. The following convention is adhered to throughout the paper: quantities marked with a tilde are defined on a plate edge or on a finite element boundary only; prescribed quantities are marked with an asterisk; the superscript T denotes the transpose of a matrix or vector. Two additional special column vectors are also required, viz:

$$\left.\begin{aligned} \mathbf{E} &= (E_x E_y E_z)^T, \\ \tilde{\mathbf{E}} &= (E_x E_y \tilde{E}_z)^T, \end{aligned}\right\} \quad (2\text{-}2)$$

whose components are

$$\left.\begin{aligned} E_x &= \frac{\partial N_x}{\partial x} + \frac{\partial N_{xy}}{\partial y}, \\ E_y &= \frac{\partial N_y}{\partial y} + \frac{\partial N_{xy}}{\partial x}, \\ E_z &= \bar{E}_z + \frac{\partial}{\partial x}\left(N_x \frac{\partial W}{\partial x} + N_{xy} \frac{\partial W}{\partial y}\right) + \frac{\partial}{\partial y}\left(N_y \frac{\partial W}{\partial y} + N_{xy} \frac{\partial W}{\partial x}\right), \\ \bar{E}_z &= \frac{\partial^2 M_x}{\partial x^2} + 2\frac{\partial^2 M_{xy}}{\partial x \partial y} + \frac{\partial^2 M_y}{\partial y^2}. \end{aligned}\right\} \tag{2-3}$$

A complete list of the symbols used in the text is given in the Notation.

Adopting the above conventions, the generalized complementary energy functional[11] for finite element analysis of a plate of area A, with kinematic conditions prescribed on the part $\mathscr{C}_k$ of its edge and applied tractions on the part $\mathscr{C}_T$ of its edge, is written concisely as

$$\Pi_{FE} = \tfrac{1}{2}\int\int_A \mathbf{M}^T \mathscr{K} \mathbf{M}\, dA + \tfrac{1}{2}\int\int_A \mathbf{N}^T \mathscr{F} \mathbf{N}\, dA + \tfrac{1}{2}\int\int_A \theta^T \mathscr{B} \theta\, dA - \int_{\mathscr{C}_k} \mathbf{R}^T \mathbf{U}^*\, ds$$
$$+ \iint_A (\mathbf{E} + \mathbf{p}^*)\mathbf{U}\, dA - \int_{\mathscr{C}_T} (\mathbf{R} - \mathbf{R}^*)^T \tilde{\mathbf{U}}\, ds. \tag{2-4}$$

The components of the matrices $\mathscr{K}$ and $\mathscr{F}$ contain the elastic and geometric properties of the plate relevant to the bending and stretching actions respectively. The matrix $\mathscr{B}$ is given by

$$\mathscr{B} = \begin{bmatrix} N_x & N_{xy} \\ N_{xy} & N_y \end{bmatrix}. \tag{2-5}$$

We now consider that the functional of eqn (2-4) applies to a single triangular element of area Δ which forms part of a finite element mesh completely covering the whole plate. The boundary $\mathscr{C}$ of the element is assumed to consist of two parts, denoted $\mathscr{C}_k$ and $\mathscr{C}_T$ as above, where displacements and tractions are prescribed respectively. The part of the element boundary $\mathscr{C}_T$ is taken to include the boundaries common to adjacent elements inside the plate on the basis that they are also concerned with the transmission of tractions. The contribution of a single element to the total functional for the plate is therefore

$$\pi_e = \tfrac{1}{2}\int\int_\Delta \mathbf{M}^T \mathscr{K} \mathbf{M}\, d\Delta + \tfrac{1}{2}\int\int_\Delta \mathbf{N}^T \mathscr{F} \mathbf{N}\, d\Delta + \tfrac{1}{2}\iint_\Delta \theta^T \mathscr{B} \theta\, d\Delta - \oint_{\mathscr{C}} \mathbf{R}^T \tilde{\mathbf{U}}\, ds$$
$$+ \int_{\mathscr{C}_T} \mathbf{R}^{*T} \tilde{\mathbf{U}}\, ds + \iint_\Delta (\mathbf{E} + \mathbf{p}^*)^T \mathbf{U}\, dA + \int_{\mathscr{C}_k} \mathbf{R}^T (\tilde{\mathbf{U}} - \mathbf{U}^*) ds, \tag{2-6}$$

where the coordinate s is measured anti-clockwise around the element boundary $\mathscr{C}$.

The functional for a standard hybrid stress model follows from eqn (2-6) by selecting finite element trial functions which satisfy the differential equations of equilibrium inside the element and the prescribed displacement conditions on the element boundary, i.e.

$$\left.\begin{aligned} \mathbf{E} + \mathbf{p}^* &= 0 \quad \text{in } \Delta \\ \tilde{\mathbf{U}} &= \mathbf{U}^* \quad \text{on } \mathscr{C}. \end{aligned}\right\} \tag{2-7}$$

However, the choice of suitable trial functions to satisfy the first of eqns (2-7) presents some difficulties (see Tabarrok and Gass[7]) and it is preferable to follow the alternative approach first adopted for initial buckling[8, 9]. We require the Green's formula

$$\iint_{\Delta} \mathbf{E}^T \mathbf{U}\, d\Delta = \iint_{\Delta} \bar{\mathbf{E}}^T\, d\Delta - \iint_{\Delta} \theta^T \mathscr{B} \theta\, d\Delta + \oint_{\mathscr{C}} \left(N_n \frac{\partial W}{\partial n} + N_{nt} \frac{\partial W}{\partial s} \right) W\, ds \tag{2-8}$$

and we recall[11] that the total shear force along a boundary is

$$V_n = K_n + N_n \frac{\partial W}{\partial n} + N_{nt} \frac{\partial W}{\partial s}, \tag{2-9}$$

where K_n is the Kirchhoff shear force. Introducing the column vectors $\bar{\mathbf{R}}$ and $\bar{\mathbf{E}}$ defined in eqns (2-1) and (2-2) and using eqns (2-8) and (2-9), an alternative form for eqn (2-6) is found to be

$$\begin{aligned} \pi_e = {} & \tfrac{1}{2} \iint_{\Delta} \mathbf{M}^T \mathscr{K} \mathbf{M}\, d\Delta + \tfrac{1}{2} \iint_{\Delta} \mathbf{N}^T \mathscr{F} \mathbf{N}\, d\Delta - \tfrac{1}{2} \iint_{\Delta} \theta^T \mathscr{B} \theta\, dA - \oint_{\mathscr{C}} \bar{\mathbf{R}}^T \tilde{\mathbf{U}}\, ds \\ & + \int_{\mathscr{C}_T} \mathbf{R}^{*T} \tilde{\mathbf{U}}\, ds + \iint_{\Delta} (\bar{\mathbf{E}} + \mathbf{p}^*)^T \mathbf{U}\, d\Delta + \int_{\mathscr{C}_K} \mathbf{R}^T (\tilde{\mathbf{U}} - \mathbf{U}^*)\, ds \\ & + \oint_{\mathscr{C}} \left(N_n \frac{\partial W}{\partial n} + N_{nt} \frac{\partial W}{\partial s} \right) (W - \tilde{W})\, ds. \end{aligned} \tag{2-10}$$

Equation (2-10) is reduced to its simplest form by selecting finite element trial functions which satisfy the constraint equations

$$\left.\begin{aligned} \bar{\mathbf{E}} &= 0 \quad \text{in } \Delta, \\ \tilde{\mathbf{U}} &= \mathbf{U}^* \quad \text{on } \mathscr{C}_K, \\ W &= \tilde{W} \quad \text{on } \mathscr{C}. \end{aligned}\right\} \tag{2-11}$$

The result of this reduction is

$$\begin{aligned} \pi_e = {} & \tfrac{1}{2} \iint_{\Delta} \mathbf{M}^T \mathscr{K} \mathbf{M}\, d\Delta + \tfrac{1}{2} \iint_{\Delta} \mathbf{N}^T \mathscr{F} \mathbf{N}\, d\Delta - \tfrac{1}{2} \iint_{\Delta} \theta^T \mathscr{B} \theta\, d\Delta - \oint_{\mathscr{C}} \bar{\mathbf{R}}^T \tilde{\mathbf{U}}\, ds \\ & + \int_{\mathscr{C}_T} \mathbf{R}^{*T} \tilde{\mathbf{U}}\, ds + \iint_{\Delta} \mathbf{p}^{*T} \mathbf{U}\, d\Delta. \end{aligned} \tag{2-12}$$

The variational functional used in the present paper for the finite element analysis of the large displacement bending and post-buckling of thin plates is obtained by summing over all the elements the quantities π_e given in eqn (2-12). This equation also reduces either to the functional previously used for the finite element analysis of the small displacement bending of plates[6] if we put $\mathbf{N} = 0$ and $X^* = Y^* = 0$, or to the functional used for the finite element analysis of plate buckling[8, 9] if we take the components of $\mathbf{N}$ as prescribed quantities together with $\mathbf{p}^* = 0$.

3. FINITE ELEMENT IDEALIZATION

The successful calculation of the nonlinear elastic bending and post-buckling of thin plates requires a finite element idealization which can represent satisfactorily the specific physical actions associated with large displacement behaviour. These include rigid body movements,

simple states of stretching and bending and boundary layer effects. Some of the problems in selecting suitable trial functions are noted in a previous publication[12]. In particular, it is conjectured that an important criterion for the trial functions is to recover exactly all deformation states involving only constant values of strain, curvature and twist. This is proposed as a practical requirement for accurate finite element analysis if mesh idealizations of a convenient size are to be used to best advantage. It is an extension of the well-known "constant strain" criterion in linear elasticity which is often stated[13] as a necessary condition for convergence to the exact solution with refinement of the finite element mesh.

Consider the large displacement bending of a thin plate. The membrane strains ϵ_x, ϵ_y and γ_{xy} are calculated from the membrane displacements U and V and normal displacement W by the nonlinear relationships

$$\left.\begin{aligned} \epsilon_x &= \frac{\partial U}{\partial x} + \frac{1}{2}\left(\frac{\partial W}{\partial x}\right)^2, \\ \epsilon_y &= \frac{\partial V}{\partial y} + \frac{1}{2}\left(\frac{\partial W}{\partial y}\right)^2, \\ \gamma_{xy} &= \frac{\partial V}{\partial x} + \frac{\partial U}{\partial y} + \frac{\partial W}{\partial x}\frac{\partial W}{\partial y}. \end{aligned}\right\} \tag{3-1}$$

In the case of inextensional bending the membrane strains are zero and it follows that the normal displacement W satisfies an equation obtained by eliminating U and V from eqn (3-1), viz:

$$\left(\frac{\partial^2 W}{\partial x \partial y}\right)^2 - \frac{\partial^2 W}{\partial x^2}\frac{\partial^2 W}{\partial y^2} = 0. \tag{3-2}$$

This is the equation of a developable surface. The curvatures κ_x, κ_y and twist κ_{xy} are obtained from the normal displacements using the equations

$$\left.\begin{aligned} \kappa_x &= -\frac{\partial^2 W}{\partial x^2}, \\ \kappa_y &= -\frac{\partial^2 W}{\partial y^2}, \\ \kappa_{xy} &= -\frac{\partial^2 W}{\partial x \partial y}. \end{aligned}\right\} \tag{3-3}$$

They are independent of the membrane strains provided eqn (3-2) holds, i.e.

$$\kappa_{xy}^2 - \kappa_x \kappa_y = 0. \tag{3-4}$$

The general solution of eqn (3-4) is a two-parameter family of curvatures and twist

$$\left.\begin{aligned} \kappa_x &= \kappa \sin^2 \phi, \\ \kappa_y &= \kappa \cos^2 \phi, \\ \kappa_{xy} &= \kappa \sin \phi \cos \phi, \end{aligned}\right\} \tag{3-5}$$

where ϕ is the angle between the generators of the associated developable surface and the x-axis (see Ref. [11]) and where κ is the non-zero principal curvature.

It follows from Ref. [12] that all admissible states of constant strain, curvature and twist are obtained from the following polynomial distributions of normal displacement W and membrane displacement U, V viz:

$$\left.\begin{aligned} W &= a_1 + a_2 x + a_3 y - \tfrac{1}{2}(k_{11}x^2 + 2k_{12}xy + k_{22}y^2), \\ U &= a_4 + (e_{11} - \tfrac{1}{2}a_2^2)x + [a_5 + \tfrac{1}{2}(e_{12} - a_2 a_3)]y + \tfrac{1}{2}a_2(k_{11}x^2 + 2k_{12}xy + k_{22}y^2) \\ &\quad - \tfrac{1}{6}(k_{11}^2 x^3 + 3k_{11}k_{12}x^2 y + 3k_{12}^2 xy^2 + k_{12}k_{22}y^3), \\ V &= a_6 - [a_5 - \tfrac{1}{2}(e_{12} - a_2 a_3)]x + (e_{22} - \tfrac{1}{2}a_3^2)y + \tfrac{1}{2}a_3(k_{11}x^2 + 2k_{12}xy + k_{22}y^2) \\ &\quad - \tfrac{1}{6}(k_{11}k_{12}x^3 + 3k_{12}^2 x^2 y + 3k_{12}k_{22}xy^2 + k_{22}^2 y^3), \end{aligned}\right\} \tag{3-6}$$

where e_{11}, e_{22}, e_{12} are independent constant membrane strains and where k_{11}, k_{22} are independent constant curvatures with the constant twist $k_{12} = \pm\sqrt{(k_{11}k_{22})}$ to ensure satisfaction of the inextensional condition of eqn (3-2). The coefficients a_i $(i = 1, \ldots, 6)$ characterize the six rigid body movements of the plate.

It is difficult to devise an exhaustive series of simple tests to verify that the trial functions of a finite element model can represent the polynomial displacements of eqns (3-6), because many of the terms are quadratic in the coefficients a_i, e_{ij} and k_{ij}. However, a useful practical procedure to test that all the terms with linear coefficients are included in the trial functions is to attempt to recover the six rigid body movements of a plate and the six unit deformation states defined in the following Table:

Table 1.

Unit states	Components of strain, curvature and twist						Mode of deformation
	ϵ_x	ϵ_y	γ_{xy}	κ_x	κ_y	κ_{xy}	
1	1	0	0	0	0	0	
2	0	1	0	0	0	0	Pure stretching
3	0	0	1	0	0	0	
4	0	0	0	1	0	0	
5	0	0	0	0	1	0	Inextensional bending
6	0	0	0	1	1	±1	

Unit deformation states 1, 2 and 3 relate to the familiar constant strain criterion of linear elasticity associated with pure stretching action. Unit deformation states 4, 5 and 6 are obtained from eqns (3-5) with $\kappa = 1, 1, 2$ and $\phi = \pi/2, 0, \pm\pi/4$ respectively; exact recovery of these inextensional bending actions is a necessary condition for the trial functions to represent any state of constant curvature and twist independently from the membrane strains.

3.1 *Basic trial functions*

The basic finite element trial functions are selected to satisfy the constraint equations (2-11). They correspond exactly to those used previously for the analysis of plate buckling[8, 9] and large deflections of thin elastic structures[10]. Separate assumptions are made for the membrane stress resultants, the bending and twisting moments and the normal and membrane displacements. All displacements are defined separately inside each element and on the element boundary.

The connection quantities are taken as the values of displacements and derivatives at the corners of a triangular element. This gives the most efficient computational topology for a finite element scheme. The connection quantities are the components of the column vectors

$$\left.\begin{aligned} q_\alpha &= \left(W_1 \frac{\partial W_1}{\partial x}\frac{\partial W_1}{\partial y}\, W_2 \frac{\partial W_2}{\partial x}\frac{\partial W_2}{\partial y}\, W_3 \frac{\partial W_3}{\partial x}\frac{\partial W_3}{\partial y}\right)^T, \\ q_\beta &= (U_1 V_1 U_2 V_2 U_3 V_3)^T, \end{aligned}\right\} \tag{3-7}$$

where the subscripts 1, 2, 3 refer to the values at the three corners of a triangle with coordinates (x_1, y_1), (x_2, y_2) and (x_3, y_3) respectively. The displacement constraint in eqn $(2.11)_2$ is enforced by prescribing the values of the connection quantities on the boundary $\mathscr{C}_\kappa$.

The interior normal displacement $W(x, y)$ is defined as

$$W = P_\alpha{}^T q_\alpha, \tag{3-8}$$

where the nine components of the vector P_α are the cubic polynomials used by Bazeley *et al.* [14]. The first three components of this vector are written as

$$\left.\begin{aligned} P_\alpha{}^1 &= \xi_1 + \xi_1{}^2\xi_2 + \xi_1{}^2\xi_3 - \xi_1\xi_2{}^2 - \xi_1\xi_3{}^2, \\ P_\alpha{}^2 &= (x_2 - x_1)(\xi_1{}^2\xi_2 + \tfrac{1}{2}\xi_1\xi_2\xi_3) - (x_1 - x_3)(\xi_3\xi_1{}^2 + \tfrac{1}{2}\xi_1\xi_2\xi_3), \\ P_\alpha{}^3 &= (y_2 - y_1)(\xi_1{}^2\xi_2 + \tfrac{1}{2}\xi_1\xi_2\xi_3) - (y_1 - y_3)(\xi_3\xi_1{}^2 + \tfrac{1}{2}\xi_1\xi_2\xi_3), \end{aligned}\right\} \tag{3-9}$$

where the triangular coordinates are

$$\begin{bmatrix}\xi_1\\ \xi_2\\ \xi_3\end{bmatrix} = \frac{1}{2\Delta}\begin{bmatrix}(x_2y_3 - x_3y_2) & (y_2 - y_3) & (x_3 - x_2)\\ (x_3y_1 - x_1y_3) & (y_3 - y_1) & (x_1 - x_3)\\ (x_1y_2 - x_2y_1) & (y_1 - y_2) & (x_2 - x_1)\end{bmatrix}\begin{bmatrix}1\\ x\\ y\end{bmatrix}. \tag{3-10}$$

The remaining six components of the vector P_α are found by cyclic permutation of the subscripts 1, 2, 3. The normal displacement on the typical element side $1 \to 2$ of length l_{12} is assumed to be

$$\begin{aligned} \tilde{W}(s) = &\left[1 - 3\left(\frac{s}{l_{12}}\right)^2 + 2\left(\frac{s}{l_{12}}\right)^3\right] W_1 + l_{12}\left[\left(\frac{s}{l_{12}}\right)^2 - 2\left(\frac{s}{l_{12}}\right)^2 + \left(\frac{s}{l_{12}}\right)^1\right]\frac{\partial W_1}{\partial s} \\ &+ \left[3\left(\frac{s}{l_{12}}\right)^2 - 2\left(\frac{s}{l_{12}}\right)^3\right] W_2 - l_{12}\left[\left(\frac{s}{l_{12}}\right)^2 - \left(\frac{s}{l_{12}}\right)^3\right]\frac{\partial W_2}{\partial s}, \end{aligned} \tag{3-11}$$

and the derivative in the direction n of the outward normal to the side is taken as

$$\frac{\partial \tilde{W}}{\partial n}(s) = \left(1 - \frac{s}{l_{12}}\right)\frac{\partial W_1}{\partial n} + \left(\frac{s}{l_{12}}\right)\frac{\partial W_2}{\partial n}. \tag{3-12}$$

The directional derivatives in eqns (3-11) and (3-12) are given by

$$\left.\begin{aligned} \frac{\partial}{\partial s} &= -\sin\gamma_{12}\frac{\partial}{\partial x} + \cos\gamma_{12}\frac{\partial}{\partial y}, \\ \frac{\partial}{\partial n} &= \cos\gamma_{12}\frac{\partial}{\partial x} + \sin\gamma_{12}\frac{\partial}{\partial y}, \end{aligned}\right\} \tag{3-13}$$

where the angle γ_{12} lies between the direction n and the x-axis.

The trial functions assumed in eqns (3-11) and (3-12) for the normal displacement $\tilde{W}$ and the normal derivative $\partial\tilde{W}/\partial n$ are expressed in terms of the vector of connection quantities q_α, given in eqn (3-7), using eqns (3-13). This ensures satisfaction of the compatibility condition $W = \tilde{W}$ for the cubic normal displacement on an element boundary $\mathscr{C}$, as required by the constraint eqn $(2\text{-}11)_3$. But the linear normal derivative $\partial\tilde{W}/\partial n$ is not compatible with the quadratic distribution which is calculated from the interior normal displacement defined in eqn (3-8). Compatibility of normal derivatives is satisfied as a "best-fit" by virtue of the generalized variational principle, given in Ref. [11], which is used to formulate the variational equations in Section 4.

The bending and twisting moments are assumed to be linear functions with coefficients α_i $(i = 1, \ldots, 9)$:

$$\left.\begin{aligned} M_x &= \alpha_1 + \alpha_2 x + \alpha_3 y, \\ M_y &= \alpha_4 + \alpha_5 x + \alpha_6 y, \\ M_{xy} &= \alpha_7 + \alpha_8 x + \alpha_9 y, \end{aligned}\right\} \tag{3-14}$$

which clearly satisfy the required constraint condition $(2\text{-}11)_1$.

The above choice for the trial functions to represent the bending action of a plate is a well-tried combination already used for the analysis of the small displacement bending[6] and buckling[8, 9] of plates. It ensures that the finite element model is free from spurious kinematic modes[15, 16]. Moreover, this combination of trial functions can represent exactly a general quadratic distribution of normal displacement. In the context of small displacement theory this idealization can recover any state of constant curvature and twist. However, the successful recovery of unit deformation states 4–6 in Table 1 for constant curvatures and twist associated with large displacement bending requires a careful selection of trial functions for the stretching action.

Here, the basic trial functions for stretching are chosen to give the simplest finite element idealization without regard for the exact recovery of any deformation state with constant curvatures and twist. The interior displacements $U(x, y)$, $V(x, y)$ are taken as linear functions

$$\begin{bmatrix} U \\ V \end{bmatrix} = \begin{bmatrix} \xi_1 & 0 & \xi_2 & 0 & \xi_3 & 0 \\ 0 & \xi_1 & 0 & \xi_2 & 0 & \xi_3 \end{bmatrix} q_\beta, \tag{3-15}$$

where ξ_i are the triangular coordinates defined in eqn (3-10) and q_β is the vector of connection quantities in eqn $(3\text{-}7)_2$. The boundary displacements $\bar{U}_n(s)$, $\bar{U}_t(s)$ in the directions of the outward normal n and the tangent t are defined along the typical side $1 \rightarrow 2$ as

$$\left.\begin{aligned} \bar{U}_n(s) &= \left(1 - \frac{s}{l_{12}}\right) U_{n_1} + \left(\frac{s}{l_{12}}\right) U_{n_2}, \\ \bar{U}_t(s) &= \left(1 - \frac{s}{l_{12}}\right) U_{t_1} + \left(\frac{s}{l_{12}}\right) U_{t_2}. \end{aligned}\right\} \tag{3-16}$$

At node 1, the quantities U_{n_1} and U_{t_1} are transformed by

$$\left.\begin{aligned} U_{n_1} &= \cos \gamma_{12} U_1 + \sin \gamma_{12} V_1, \\ U_{t_1} &= -\sin \gamma_{12} U_1 + \cos \gamma_{12} V_1, \end{aligned}\right\} \tag{3-17}$$

where the displacements U_1 and V_1 are components of the vector of connection quantities q_α. The interior membrane displacement and the boundary displacements are therefore compatible at the element boundary.

The trail functions for the stress resultants are assumed to have constant values β_i $(i = 1, 2, 3)$, viz:

$$\begin{aligned} N_x &= \beta_1, \\ N_y &= \beta_2, \\ N_{xy} &= \beta_3, \end{aligned} \tag{3-18}$$

thus satisfying the constraint eqn $(2\text{-}11)_1$.

Of course, this type of idealization for the stretching action with compatible linear membrane displacements and constant stress resultants is tantamount to using the well-known "constant strain triangle". But the present formulation is most convenient for subsequent developments in this paper where the boundary displacements are adapted to permit recovery of the polynomial distributions defined in eqn (3-6).

The particular physical actions which can be represented exactly by the basic finite element trial functions involve linear distributions of normal and membrane displacements. They are itemized as follows:

(1) two rigid body displacements and a rigid body rotation in the plane of a plate,

(2) a rigid body displacement and two rigid body rotations associated with movements normal to the plane of a plate,

(3) three independent constant states of membrane strain.

It is emphasized that a finite element model employing the above basic trial functions cannot represent constant states of curvature and twist which are independent of the membrane strains. It fails the test procedure described in Section 3 because the unit deformation states 4, 5 and 6 of Table 1 cannot be recovered exactly.

3.2 *Augmented membrane displacements*

It is necessary for the displacement trial functions to represent exactly the polynomials of eqn (3-6) in order to recover all admissible states of constant strain, curvature and twist. While it is clear that the trial functions for the normal displacement in eqns (3-8), (3-11) and (3-12) are adequate in this respect, it is equally clear that those for the membrane displacements in eqns (3-15) and (3-16) are inadequate. The latter must be replaced by new expressions which include the cubic polynomials of eqns $(3\text{-}6)_2$ and $(3\text{-}6)_3$. But it is known[12] that there are undesirable algebraic difficulties in deriving two-dimensional cubic trial functions for the membrane displacements. Fortunately, trial functions for the interior membrane displacements U and V are required only if there are prescribed body forces X^* and Y^* in eqn (2-12); and these can be satisfactorily dealt with by the alternative methods described in Section 3.4. It is therefore sufficient to address the simpler problem of augmenting the one-dimensional linear distributions of membrane displacement given in eqns (3-16).

Consider a line, lying in the (x, y) plane of a plate, which is orientated along the y-axis so that the x-axis is the direction of the normal to the line. We assume that the membrane strains are constant and we solve eqns (3-1) for the membrane displacements U and V in the following way: differentiate eqn $(3\text{-}1)_2$ with respect to x and eqn $(3\text{-}1)_3$ with respect to y to obtain

$$\left.\begin{aligned} \frac{\partial^2 V}{\partial x \partial y} + \frac{\partial W}{\partial y}\frac{\partial^2 W}{\partial x \partial y} &= 0, \\ \frac{\partial^2 V}{\partial x \partial y} + \frac{\partial^2 U}{\partial y^2} + \frac{\partial W}{\partial y}\frac{\partial^2 W}{\partial x \partial y} + \frac{\partial W}{\partial x}\frac{\partial^2 W}{\partial y^2} &= 0, \end{aligned}\right\} \tag{3-19}$$

and subtract these two equations to give

$$\frac{\partial^2 U}{\partial y^2} + \frac{\partial W}{\partial x}\frac{\partial^2 W}{\partial y^2} = 0. \tag{3-20}$$

Equations (3-20) and $(3\text{-}1)_2$ therefore define U and V as functions of y along the line in terms of the normal displacement W and its normal derivative $\partial W/\partial x$. Now, if the line is taken to coincide with a side of a triangular finite element, it follows that the boundary displacements $\tilde{U}_n(s)$, $\tilde{U}_t(s)$ and $\tilde{W}(s)$ which permit constant strains to exist independently of the bending deformations satisfy the equations

$$\left.\begin{aligned} \frac{\partial^2 \tilde{U}_n}{\partial s^2} + \frac{\partial \tilde{W}}{\partial n}\frac{\partial^2 \tilde{W}}{\partial s^2} &= 0, \\ \frac{\partial \tilde{U}_t}{\partial s} + \frac{1}{2}\left(\frac{\partial \tilde{W}}{\partial s}\right)^2 &= C, \end{aligned}\right\} \tag{3-21}$$

where C is a constant strain along the element side and where n and s are the coordinates in the directions of the exterior normal and the tangent respectively. Equations (3-21) are easily integrated to determine the membrane displacements $\tilde{U}_n$ and $\tilde{U}_t$ corresponding to any line distribution of normal displacement $\tilde{W}$ and normal derivative $\partial \tilde{W}/\partial n$. In particular, for constant curvatures and twist, the normal derivative is given by eqn (3-12) and the first and second

derivatives with respect to s are given by

$$\left.\begin{aligned}\frac{\partial \tilde{W}}{\partial s} &= \left(1-\frac{s}{l_{12}}\right)\frac{\partial W_1}{\partial s}+\left(\frac{s}{l_{12}}\right)\frac{\partial W_2}{\partial s},\\ \frac{\partial^2 \tilde{W}}{\partial s^2} &= -\frac{1}{l_{12}}\left(\frac{\partial W_1}{\partial s}-\frac{\partial W_2}{\partial s}\right),\end{aligned}\right\} \tag{3-22}$$

where the suffices 1 and 2 refer to the ends of the typical side $1\rightarrow 2$. Integration of eqn (3-21) and evaluation of the three constants of integration, together with the constant C, in terms of the end-values then provides the augmented membrane displacements on the element boundary:

$$\begin{aligned}\tilde{U}_n(s) &= \left(1-\frac{s}{l_{12}}\right)U_{n_1}+\left(\frac{s}{l_{12}}\right)U_{n_2}+\frac{l_{12}}{6}\left(\frac{s}{l_{12}}\right)\left(1-\frac{s}{l_{12}}\right)\left[\left(2\frac{\partial W_1}{\partial n}+\frac{\partial W_2}{\partial n}\right)\right.\\ &\quad\left.+\left(\frac{\partial W_2}{\partial n}-\frac{\partial W_1}{\partial n}\right)\left(\frac{s}{l_{12}}\right)\right]\left(\frac{\partial W_2}{\partial s}-\frac{\partial W_1}{\partial s}\right),\\ \tilde{U}_t(s) &= \left(1-\frac{s}{l_{12}}\right)U_{t_1}+\left(\frac{s}{l_{12}}\right)U_{t_2}+\frac{l_{12}}{6}\left(\frac{s}{l_{12}}\right)\left(1-\frac{s}{l_{12}}\right)\left[\left(2\frac{\partial W_1}{\partial s}+\frac{\partial W_2}{\partial s}\right)\right.\\ &\quad\left.+\left(\frac{\partial W_2}{\partial s}-\frac{\partial W_1}{\partial s}\right)\left(\frac{s}{l_{12}}\right)\right]\left(\frac{\partial W_2}{\partial s}-\frac{\partial W_1}{\partial s}\right).\end{aligned} \tag{3-23}$$

These are expressed in terms of the connection quantities in eqns (3-7) using the transformations of eqns (3-13) and (3-17).

When eqns (3-23) are used for the membrane boundary displacements, instead of eqns (3-16), the resulting finite element model can recover all states of constant strain, curvature and twist associated with eqns (3-6). It is found that the finite element trial functions pass the test procedure described previously, i.e. they permit exact recovery of six rigid body movements and the six unit deformation states defined in Table 1.

3.3 *Generalized forces and displacements*

It facilitates our finite element analysis if the concept of generalized forces and displacements is introduced. Referring to the variational functional (2-12), we consider that the line integral around the element boundary $\mathscr{C}$ comprises two parts I_α and I_β, thus

$$\left.\begin{aligned}&\oint_{\mathscr{C}} \bar{R}^T\tilde{U}\,ds = I_\alpha + I_\beta,\\ &\text{where}\\ &I_\alpha = \sum_{N=1}^{3} R_N W_N + \oint_{\mathscr{C}} K_n\tilde{W}\,ds - \oint_{\mathscr{C}} M_n\frac{\partial \tilde{W}}{\partial n}\,ds,\\ &\text{and}\\ &I_\beta = \oint_{\mathscr{C}} N_n\tilde{U}_n\,ds + \oint_{\mathscr{C}} N_{nt}\tilde{U}_t\,ds.\end{aligned}\right\} \tag{3-24}$$

In eqn (3-24)$_2$, the concentrated "corner" forces R_N, the Kirchhoff shear force K_n and the

normal bending moment M_n along a typical side $1 \rightarrow 2$ are given by

$$\left.\begin{aligned} R_N &= M_{nt}^{+} - M_{nt}^{-}, \\ K_n &= \frac{\partial M_n}{\partial n} + 2\frac{\partial M_{nt}}{\partial s}, \\ M_n &= M_x \cos^2 \gamma_{12} + M_y \sin^2 \gamma_{12} + M_{xy} \sin 2\gamma_{12}, \end{aligned}\right\} \tag{3-25}$$

where the superscripts + and − refer to the concurrent sides at an element corner N and where the twisting moment

$$M_{nt} = \tfrac{1}{2}(M_y - M_x) \sin 2\gamma_{12} + M_{xy} \cos 2\gamma_{12}. \tag{3-26}$$

For a linear distribution of bending and twisting moments, such as eqn (3-14), we define

$$\left.\begin{aligned} M_n &= \left(1 - \frac{s}{l_{12}}\right) M_n^{12} + \left(\frac{s}{l_{12}}\right) M_n^{21}, \\ K_n &= K_n^{12}, \end{aligned}\right\} \tag{3-27}$$

where the quantities M_n^{12}, M_n^{21} and K_n^{21} are generalized forces. Including the corner forces R_N, the triangular element has a total of 12 generalized forces which are given by the column vector

$$G_\alpha = (R_1 K_n^{12} M_n^{12} M_n^{21} R_2 K_n^{23} M_n^{23} M_n^{32} R_3 K_n^{31} M_n^{31} M_n^{13})^T. \tag{3-28}$$

Substituting eqns (3-28) into the eqn $(3\text{-}24)_2$ for I_α gives

$$I_\alpha = G_\alpha{}^T g_\alpha, \tag{3-29}$$

where the generalized displacements corresponding to the generalized forces of eqn (3-28) are the components of a column vector g_α, thus

$$\left.\begin{aligned} g_\alpha{}^1 &= W_1, & g_\alpha{}^2 &= \int_0^{l_{12}} \tilde{W}\, ds, \\ g_\alpha{}^3 &= \int_0^{l_{12}} \left(1 - \frac{s}{l_{12}}\right) \frac{\partial \tilde{W}}{\partial n}\, ds, & g_\alpha{}^4 &= \int_0^{l_{12}} \left(\frac{s}{l_{12}}\right) \frac{\partial \tilde{W}}{\partial n}\, ds, \quad \text{etc.} \end{aligned}\right\} \tag{3-30}$$

Similarly, the normal and shearing stress resultants along the typical side $1 \rightarrow 2$ are given by

$$\left.\begin{aligned} N_n &= N_x \cos^2 \gamma_{12} + N_y \sin^2 \gamma_{12} + N_{xy} \sin 2\gamma_{12}, \\ N_{nt} &= \tfrac{1}{2}(N_y - N_x) \sin 2\gamma_{12} + N_{xy} \cos 2\gamma_{12}, \end{aligned}\right\} \tag{3-31}$$

so that the generalized forces for the constant stress resultants defined in eqn (3-18) are a total of six given by the column vector

$$G_\beta = (N_n^{12} N_{nt}^{12} N_n^{23} N_{nt}^{23} N_n^{31} N_{nt}^{31})^T. \tag{3-32}$$

The eqn $(3\text{-}24)_3$ for I_β is then

$$I_\beta = G_\beta{}^T g_\beta, \tag{3-33}$$

where the corresponding generalized displacements are the components of a column vector g_β:

$$g_\beta{}^1 = \int_0^{l_{12}} \tilde{U}_n\, ds, \quad g_\beta{}^2 = \int_0^{l_{12}} \tilde{U}_t\, ds, \quad \text{etc.} \tag{3-34}$$

The column vectors G_α and G_β are respectively related to the coefficients α_i of the bending and twisting moments in eqn (3-14) and to the coefficients β_i of the stress resultants in eqn (3-18) as follows

$$\left.\begin{aligned} G_\alpha &= B^T\alpha, \\ G_\beta &= C^T\beta. \end{aligned}\right\} \tag{3-35}$$

Here, the components of the (9×12) matrix B and the (3×6) matrix C are calculated using eqns (3-25), (3-26) and (3-31) and the column vectors α and β are

$$\left.\begin{aligned} \alpha &= (\alpha_1\alpha_2\alpha_3\alpha_4\alpha_5\alpha_6\alpha_7\alpha_8\alpha_9)^T, \\ \beta &= (\beta_1\beta_2\beta_3)^T. \end{aligned}\right\} \tag{3-36}$$

3.4 *Treatment of distributed loads*

Distributed loading on a plate is assumed to take three forms: an applied pressure $p_z^*(x, y)$ normal to the plane of the plate and two components of in-plane body force $X^*(x, y)$, $Y^*(x, y)$. These effects are included in the analysis by the integral

$$\iint_\Delta \mathbf{p}^{*T}\mathbf{U}\,d\Delta = \iint_\Delta X^*U\,dx\,dy + \iint_\Delta Y^*V\,dx\,dy + \iint_\Delta p_z^*W\,dx\,dy, \tag{3-37}$$

which appears in the functional of eqn (2-12).

In the case of the basic finite element model, described in Section 4.1, the integrals on the r.h.s. of eqn (3-37) are calculated using the trial functions for the interior displacements U, V, W given in eqns (3-15) and (3-8). However, the augmented displacements model and the equilibrium model described in Sections 4.2 and 4.3 are better treated by an alternative method which avoids the algebraic complications of two-dimensional trial functions for U and V without damaging their capability to recover the polynomial displacements of eqn (3-6). The method is valid if the prescribed body forces X^*, Y^* are derived from a potential function $\Omega(x, y)$. Fortunately, this condition applies to most types of body force which occur in practical problems, e.g. gravitational force, centrifugal force, magnetic force. Accordingly, the membrane stress resultants are re-defined as

$$\left.\begin{aligned} N_x &= \beta_1 + \Omega, \\ N_y &= \beta_2 + \Omega, \\ N_{xy} &= \beta_3, \end{aligned}\right\} \tag{3-38}$$

where the potential function Ω for the body forces is given by

$$\left.\begin{aligned} \frac{\partial\Omega}{\partial x} &= -X^*, \\ \frac{\partial\Omega}{\partial y} &= -Y^*. \end{aligned}\right\} \tag{3-39}$$

Equations (3-38) and (3-39) ensure that the equations of equilibrium in the plane of the plate are satisfied exactly by the trial functions, i.e.

$$\left.\begin{aligned} E_x + X^* &= 0, \\ E_y + Y^* &= 0, \end{aligned}\right\} \tag{3-40}$$

where E_x and E_y are given by eqns $(2\text{-}3)_1$ and $(2\text{-}3)_2$. Consequently, the first and second integrals on the r.h.s. of eqn (3-37) do not appear in the functional of eqns (2-12) and there is no

requirement for finite element representations of the interior membrane displacements U and V.

Finally, we note that the equilibrium model for stretching, described in Section 4.3, requires extra generalized displacements for the exact transmission across element boundaries of the stress resultants defined in eqn (3-38). The expressions for these generalized displacements can be derived only when the form of the potential function Ω is known.

4. MATRIX FORMULATION OF VARIATIONAL EQUATIONS

It is convenient to express the functional of eqn (2-12) in a new matrix notation before formulating the variational equations which are used in the numerical solution. For simplicity of presentation, it is assumed here that a normal pressure p_z^* is the only component of the body force applied to the plate; the in-plane components of the body force vector $\mathbf{p}^*$ are taken to be zero, i.e. $X^* = Y^* = 0$. The effect of non-zero body forces X^*, Y^* is included in the analysis by the methods described in Section 3.4.

Using eqns (3-14) and (3-18), the first two integrals of the functional are written

$$\left.\begin{aligned} \tfrac{1}{2}\iint_{\Delta} \mathbf{M}^T \mathscr{K} \mathbf{M}\, d\Delta &= \tfrac{1}{2}\alpha^T H_{\alpha\alpha}\alpha, \\ \tfrac{1}{2}\iint_{\Delta} \mathbf{N}^T \mathscr{F} \mathbf{N}\, d\Delta &= \tfrac{1}{2}\beta^T H_{\beta\beta}\beta, \end{aligned}\right\} \tag{4-1}$$

where $H_{\alpha\alpha}$ is a (9×9) matrix and $H_{\beta\beta}$ is a (3×3) matrix; the column vectors α and β are given by eqn (3-36). The third integral is defined as a scalar quantity Λ which is written in two alternative forms as follows

$$\Lambda = \tfrac{1}{2}\iint_{\Delta} \theta^T \mathscr{B} \theta\, d\Delta = \begin{cases} \tfrac{1}{2} q_\alpha{}^T N_{\beta\beta} q_\alpha, \\ \beta^T L_\alpha \end{cases} \tag{4-2}$$

where q_α is the column vector of connection quantities in eqn $(3\text{-}7)_1$ and $N_{\beta\beta}$ is a (9×9) matrix whose elements are linear functions of the stress coefficients β_i. The three components of the column vector L_α are quadratic functions of the connection quantities in q_α. The effect of the applied normal pressure is calculated using eqn (3-8) for the normal displacement; the result is

$$\iint_{\Delta} p_z^* W\, d\Delta = q_\alpha{}^T P^*, \tag{4-3}$$

where P^* is a (9×1) column vector.

The functional of eqn (2-12) is now written in matrix notation as

$$\pi_c = \tfrac{1}{2}\alpha^T H_{\alpha\alpha}\alpha + \tfrac{1}{2}\beta^T H_{\beta\beta}\beta - \Lambda - I_\alpha - I_\beta + g_\alpha{}^T G_\alpha^* + g_\beta{}^T G_\beta^* + q_\alpha{}^T P^*, \tag{4-4}$$

where the boundary integrals I_α, I_β are defined in eqns $(3\text{-}24)_2$ and $(3\text{-}24)_3$ and the generalized displacements g_α, g_β are defined in eqns (3-30) and (3-34). The column vectors G_α^*, G_β^* contain prescribed values of the generalized forces defined in eqns (3-28) and (3-32).

4.1 *Basic finite element model*

The basic trial functions of eqns (3-11), (3-12) and (3-16) are used to calculate the generalized displacements defined in eqns (3-30) and (3-34). The result is written

$$\left.\begin{aligned} g_\alpha &= Tq_\alpha, \\ g_\beta &= Sq_\beta, \end{aligned}\right\} \tag{4-5}$$

where T is a (12×9) matrix and S is a (6×6) matrix. The boundary integrals I_α and I_β are given by eqns (3-29), (3-33), (3-35) and (4-5) as

$$\left.\begin{aligned} I_\alpha &= \alpha^T(BT)q_\alpha, \\ I_\beta &= \beta^T(CS)q_\beta. \end{aligned}\right\} \tag{4-6}$$

Using eqns (4-5) and (4-6) the element functional π_e in eqn (4-4) becomes

$$\pi_e = \tfrac{1}{2}\alpha^T H_{\alpha\alpha}\alpha + \tfrac{1}{2}\beta^T H_{\beta\beta}\beta - \Lambda - \alpha^T(BT)q_\alpha - \beta^T(CS)q_\beta + q_\alpha{}^T T^T G_\alpha^* + q_\beta{}^T S^T G_\beta^* + q_\alpha{}^T P^*. \tag{4-7}$$

Considering arbitrary variations $\delta\alpha$, $\delta\beta$, δq_α and δq_β the first variation $\delta\pi_e$ is

$$\begin{aligned} \delta\pi_e = {} & \delta\alpha^T[H_{\alpha\alpha}\alpha - (BT)q_\alpha] + \delta\beta^T[H_{\beta\beta}\beta - L_\alpha - (CS)q_\beta] \\ & - \delta q_\alpha{}^T[N_{\beta\beta}q_\alpha + (BT)^T\alpha - T^T G_\alpha^* - P^*] - \delta q_\beta{}^T[(CS)^T\beta - S^T G_\beta^*]. \end{aligned} \tag{4-8}$$

The sum of the first variations $\delta\pi_e$ from all the finite elements is set to zero as required for an application of the variational principle presented in Ref. [11]. But, we recall that the variations $\delta\alpha$ and $\delta\beta$ are local to each element because the stress resultants and stress couples are assumed independently from the connection quantities; their coefficients in eqn (4-8) therefore vanish, i.e.

$$\left.\begin{aligned} H_{\alpha\alpha}\alpha &= (BT)q_\alpha \\ H_{\beta\beta}\beta &= L_\alpha + (CS)q_\beta. \end{aligned}\right\} \tag{4-9}$$

Inverting eqns (4-9) and substituting for α and β in eqn (4-8) gives an expression for $\delta\pi_e$ in terms of the vectors of connection quantities q_α and q_β only. Summing $\delta\pi_e$ over all elements e and setting the result to zero provides the variational equations for the basic finite element model, viz:

$$\left.\begin{aligned} \sum_e [(BT)^T H_{\alpha\alpha}^{-1}(BT) + N_{\beta\beta}]q_\alpha &= \sum_e \{T^T G_\alpha^* + P^*\}, \\ \sum_e [(CS)^T H_{\beta\beta}^{-1}(CS)]q_\beta &= \sum_e \{S^T G_\beta^* - (CS)^T H_{\beta\beta}^{-1} L_\alpha\}, \end{aligned}\right\} \tag{4-10}$$

where the components of the column vectors q_α and q_β are constrained to satisfy the displacement boundary conditions of eqn $(2\text{-}11)_2$. The numerical solution of these nonlinear equations is discussed in Section 5.

4.2 *Augmented displacements model*

The augmented membrane displacements of eqns (3-23) are used to calculate the generalized displacements defined in eqns (3-34). The boundary integral I_β in eqn $(4\text{-}6)_2$ than takes the expanded form

$$I_\beta = \beta^T(CS)q_\beta + \Gamma, \tag{4-11}$$

where the quantity Γ includes the extra terms to permit exact recovery of inextensional bending deformations with constant curvatures and twist. It has two alternative forms as follows

$$\Gamma = \begin{cases} \tfrac{1}{2}q_\alpha{}^T M_{\beta\beta}q_\alpha, \\ \beta^T R_\alpha. \end{cases} \tag{4-12}$$

Here, the elements of the (9×9) matrix $M_{\beta\beta}$ are linear functions of the stress coefficients β_i and

the three components of the column vector R_α are quadratic functions of the connection quantities in q_α.

Substituting eqn (4-11) into eqn (4-4) and following a similar procedure to Section 4.1 gives

$$\left.\begin{aligned} H_{\alpha\alpha}\alpha &= (BT)q_\alpha, \\ H_{\beta\beta}\beta &= (CS)q_\beta + L_\alpha + R_\alpha \end{aligned}\right\} \tag{4-13}$$

The variational equations for the augmented displacements model are

$$\left.\begin{aligned} \sum_e [(BT)^T H_{\alpha\alpha}^{-1}(BT) + N_{\beta\beta} + M_{\beta\beta} - M^*_{\beta\beta}]q_\alpha &= \sum_e \{T^T G^*_\alpha + P^*\}, \\ \sum_e [(CS)^T H_{\beta\beta}^{-1}(CS)]q_\beta &= \sum_e \{S^T G^*_\beta - (CS)^T H_{\beta\beta}^{-1}(L_\alpha + R_\alpha)\}, \end{aligned}\right\} \tag{4-14}$$

where the matrix $M^*_{\beta\beta}$ has an identical form to $M_{\beta\beta}$, but its elements contain contributions from the prescribed boundary tractions G^*_β instead of the stress coefficients β_i. The components of the column vectors q_α and q_β are again constrained to satisfy the displacement boundary conditions of eqn $(2\text{-}11)_2$. Equations (4-14) are no more difficult to solve numerically than eqns (4-10).

4.3 *Equilibrium model for stretching*

An alternative method which has been proposed[12] for recovering inextensional bending deformations involves the use of an equilibrium model for the stretching action in a plate. This approach uses generalized displacements, such as those defined in eqn (3-34), as connection quantities on the side of an element instead of the corner connection quantities defined in eqn $(3\text{-}7)_2$. The generalized displacements are point Lagrangian multipliers to enforce equilibrium of the membrane stress resultants between adjacent finite elements and to satisfy the traction boundary conditions at the plate edge. Clearly, they can take any numerical values consistent with the requirements for inextensional bending without damaging their rôle in enforcing stress equilibrium.

For an equilibrium model with constant stress resultants, as defined in eqns (3-18), the column vectors α and β are determined from

$$\left.\begin{aligned} H_{\alpha\alpha}\alpha &= (BT)q_\alpha, \\ H_{\beta\beta}\beta &= L_\alpha + Cg_\beta, \end{aligned}\right\} \tag{4-15}$$

and the appropriate variational equations are

$$\left.\begin{aligned} \sum_e [(BT)^T H_{\alpha\alpha}^{-1}(BT) + N_{\beta\beta}]q_\alpha &= \sum_e \{T^T G^*_\alpha + P^*\}, \\ \sum_e [C^T H_{\beta\beta}^{-1} C]g_\beta &= \sum_e \{G^*_\beta - C^T H_{\beta\beta}^{-1} L_\alpha\}. \end{aligned}\right\} \tag{4-16}$$

These equations become identical to eqns (4-10) if eqn $(4\text{-}5)_2$ is used to substitute for g_β in the analysis. The latter equations are also used to calculate the constraints on the components of g_β in eqn (4-16) as specified by the displacement boundary conditions of eqn $(2\text{-}11)_2$.

An equilibrium model for stretching with constant stress resultants is a natural choice for a development from the basic finite element model described in Section 4.1. But, although the element stiffness matrix $C^T H_{\beta\beta}^{-1} C$ is well-behaved, it is known that the global stiffness matrix $\sum_e C^T H_{\beta\beta} C$ can be singular even with the rigid body movements constrained. In this instance, the variational eqns $(4\text{-}16)_2$ are rank-deficient and they require special numerical techniques for solution. A physical interpretation of this behaviour is that the finite element model corresponds to a mechanism. This difficulty can be avoided completely by using a more sophisticated equilibrium model for the stretching action. Reference 17 gives details of a suitable triangular

equilibrium element with linear stresses; the generalized displacements along the typical side $1 \rightarrow 2$ are

$$\left.\begin{aligned} g_\beta^{\,1} &= \int_0^{l_{12}} \left(1 - \frac{s}{l_{12}}\right) \tilde{U}_n \, ds, \qquad g_\beta^{\,2} = \int_0^{l_{12}} \left(\frac{s}{l_{12}}\right) \tilde{U}_n \, ds, \\ g_\beta^{\,3} &= \int_0^{l_{12}} \left(1 - \frac{s}{l_{12}}\right) \tilde{U}_t \, ds, \qquad g_\beta^{\,4} = \int_0^{l_{12}} \left(\frac{s}{l_{12}}\right) \tilde{U}_t \, ds, \end{aligned}\right\} \tag{4-17}$$

where the coordinate s is measured from node 1. The relevant variational equations are identical in form to eqns (4-16) with the matrix and vector quantities re-defined in an appropriate way.

It is an unfortunate fact that the equilibrium model has connection quantities on the element sides, thus increasing the number of equations involved in a numerical solution. This alternative offers a less attractive approach for practical applications then the augmented displacements model described in Section 4.2.

5. NUMERICAL SOLUTION

In the sequel, we specifically consider the numerical solution of eqns (4-10), but the solution of eqns (4-14) and (4-16) follows a formally identical procedure. It is known from eqn (4-2) that the vector L_α is a quadratic function of the components of q_α, the vector of connection quantities associated with the bending degrees-of-freedom of an element. Equations $(4\text{-}9)_2$ and $(4\text{-}10)_2$ therefore show that the stress coefficients β_i are also quadratic functions of the components of q_α. It follows that eqn $(4\text{-}10)_1$ is a cubic polynomial function of the bending degrees-of-freedom taken from all the finite elements e, because the elements of the matrix $N_{\beta\beta}$ are linear in β_i. Now, assuming that a given finite element mesh has a total of N_T bending degrees-of-freedom x_i $(i = 1, \ldots, N_T)$, eqns (4-10) can be rewritten symbolically as

$$K_{ij}^0 x_j + \frac{\partial f}{\partial x_i} = P_i^*, \tag{5-1}$$

where f is the quartic polynomial,

$$f = \tfrac{1}{2} K_{ij}^1 x_i x_j + \tfrac{1}{4} h_{ijkl} x_i x_j x_k x_l. \tag{5-2}$$

It is to be noted that the summation convention is assumed to hold for repeated suffices $i, j, k, l = 1, \ldots, N_T$ which occur in eqns (5-1) and (5-2) and in all subsequent equations in this section. The coefficients K_{ij}^0, $K_{ij}^1 + h_{ijkl} x_k x_l$ and P_i^* form the elements of two matrices and a column vector respectively which are identified from eqn $(4\text{-}10)_1$ as

$$\left.\begin{aligned} \sum_e [(BT)^T H_{\alpha\alpha}^{-1} (BT)] &= [K_{ij}^0], \\ \sum_e [N_{\beta\beta}] &= [K_{ij}^1 + h_{ijkl} x_k x_l], \\ \sum_e \{T^T G_\alpha^* + P^*\} &= \{P_i^*\}. \end{aligned}\right\} \tag{5-3}$$

The quantities on the r.h.s. of eqns (5-3) also have the following standard interpretation: K_{ij}^0 are the elements of the linear elastic stiffness matrix for small displacement bending; K_{ij}^1 are the elements of the geometric stiffness matrix calculated from the membrane stresses in the undeformed configuration of the plate; h_{ijkl} are constant coefficients which result from the nonlinear coupling between the bending and stretching deformations of a plate; P_i^* are the components of a vector containing applied normal loading.

5.1 *Computational procedure*

Following the development described in Ref. [12], it is convenient to conceptualize the solution of eqn (5-1) as the problem of finding the stationary points of a nonlinear energy function

$$F = \tfrac{1}{2}K_{ij}^0 x_i x_j + f - P_i^* x_i. \tag{5-4}$$

Equation (5-1) thus corresponds to a position of equilibrium defined by the stationary condition $\partial F/\partial x_i = 0$. For a position of stable equilibrium the stationary value is a minimum and the Hessian matrix, given by

$$\left[\frac{\partial^2 F}{\partial x_i \partial x_j}\right] = \left[K_{ij}^0 + \frac{\partial^2 f}{\partial x_i \partial x_j}\right], \tag{5-5}$$

is positive definite.

The following numerical iterative method has been proposed [12] for calculating the unknown quantities x_i^{r+1} at the iteration $r+1$ in terms of the known quantities x_i^r at the iteration r:

$$\left[K_{ij}^0 + \rho\frac{\partial^2 f^r}{\partial x_i \partial x_j}\right] x_j^{r+1} = P_i^* - \frac{\partial f^r}{\partial x_i} + \rho\frac{\partial^2 f^r}{\partial x_i \partial x_j} x_j^r, \tag{5-6}$$

where ρ is a constant coefficient and all the partial derivatives are evaluated at the iteration r. This procedure is a generalization of Newton's method which is obtained by putting $\rho = 1$. Theoretical studies show that the value $\rho = \frac{1}{2}$ gives an iterative procedure with the valuable property of convergence to stable positions of equilibrium only.

However, the iterative procedure is not immediately suitable for numerical computation in the form of eqn (5-6). It is necessary to substitute the function f from eqn (5-2) into eqn (5-1) to get

$$[K_{ij}^0 + \rho K_{ij}^1 + 3\rho h_{ijkl} x_k^r x_l^r] x_j^{r+1} = [(\rho - 1)K_{ij}^1 + (3\rho - 1)h_{ijkl} x_k^r x_l^r] x_j^r + p_i^*. \tag{5-7}$$

A significant computational simplification is now effected by introducing the matrix

$$[K_{ij}^2] = [K_{ij}^1 + h_{ijkl} x_k x_l], \tag{5-8}$$

because it is apparent that the elements K_{ij}^2 of this matrix can be calculated in an identical way to the elements K_{ij}^1 but with current values of the membrane stresees corresponding to the deformed configuration of the plate. Equation (5-8) is then used to eliminate the term $h_{ijkl} x_k x_l$ from eqn (5-7) and the iterative procedure takes the final form

$$[K_{ij}^0 - 2\rho K_{ij}^1 + 3\rho K_{ij}^2] x_j^{r+1} = [-2\rho K_{ij}^1 + (3\rho - 1)K_{ij}^2] x_j^r + P_i^*. \tag{5-9}$$

When using eqn (5-9) it is necessary to update the elements K_{ij}^1, K_{ij}^2 and the degrees-of-freedom x_j^r at each cycle of an iterative solution. The elements K_{ij}^0 retain fixed values throughout the computations. The solution strategy for the numerical examples presented in Section 6 involves using the above iterative procedure embedded in an incremental parameter technique, but the details of this are not given here.

5.2 *Starting values for post-buckling analysis*

The analysis of the post-buckling behaviour of initially flat plates requires starting values x_i^0 for the bending degrees-of-freedom because there are no applied normal loads P_i^* on the r.h.s. of eqn (5-9). In the present paper the starting values are taken to be

$$x_i^0 = a_0 \eta_i, \tag{5-10}$$

where η_i are the components of the eigenvector η corresponding to the initial buckling mode and where the amplitude a_0 is to be determined. It is conventional to normalize the eigenvector so that $\eta_i\eta_i = 1$.

The nonlinear energy function is obtained by substituting eqn (5-10) into eqn (5-4) with $P_i^* = 0$ to get

$$F = \tfrac{1}{2}a_0^2(K_{ij}^0 + K_{ij}^1)\eta_i\eta_j + \tfrac{1}{4}a_0^4 h_{ijkl}\eta_i\eta_j\eta_k\eta_l. \tag{5-11}$$

Now, if the intensity of the applied loading in the plane of the plate is μ times the critical value for initial buckling, we have

$$(\mu K_{ij}^0 + K_{ij}^1)\eta_j = 0, \tag{5-12}$$

and it follows from eqn (5-11) that

$$F = \tfrac{1}{2}a_0^2(1-\mu)K_{ij}^0\eta_i\eta_j + \tfrac{1}{4}a_0^4 h_{ijkl}\eta_i\eta_j\eta_k\eta_l. \tag{5-13}$$

The values of a_0 at which F takes stationary values are given by

$$\frac{\partial F}{\partial a_0} = a_0[(1-\mu)K_{ij}^0\eta_i\eta_j + a_0^2 h_{ijkl}\eta_i\eta_j\eta_k\eta_l] = 0. \tag{5-14}$$

Appropriate values for the amplitude a_0 are the solutions of eqn (5-14), viz: either

$$a_0 = 0,$$

or

$$a_0^2 = (\mu - 1)\frac{K_{ij}^0\eta_i\eta_j}{h_{ijkl}\eta_i\eta_j\eta_k\eta_l}. \tag{5-15}$$

The value $a_0 = 0$ corresponds to $\mu \leq 1$, i.e. the applied loading is equal to or less than the critical value, and the plate remains flat. For post-buckling problems we have $\mu > 1$ and a_0 is calculated from eqn $(5\text{-}15)_2$, noting the computational simplification for $h_{ijkl}\eta_k\eta_l$ given by eqn (5-8). The value of μ which corresponds to the applied loading is obtained, together with the eigenvector components η_i, by an eigenvalue solution of eqn (5-12) using the method described in Ref. [9].

6. NUMERICAL EXAMPLES

The numerical examples are selected to provide a comparison between the basic finite element model and the augmented displacements model presented in Sections 4.1 and 4.2 respectively. The examples include various kinds of elastic behaviour typical of the large displacement bending and post-buckling of thin plates. They are designed to investigate the effects of including simple inextensional bending deformations in the finite element trial functions. Both finite element models have identical connection quantities and hence there is no significant difference in the computing times required for assembling and solving the finite element equations during the iterative solution.

6.1 *Study of convergence with mesh refinement*

The convergence characteristics of the two finite element models are studied using alternative mesh refinements for a simple plate problem with an exact analytic solution. The data for the problem are given in Fig. 1. There are no displacement constraints in the plane of the plate except to restrain rigid body movements. The mid-plane of the plate is bent into a cylindrical surface, with generators parallel to the clamped edge, by a constant shear force per unit length V_x^* applied at one end. A linear distribution of normal bending moment per unit length $M_y = \nu M_x$ is required along the remaining two edges to give the correct boundary conditions for the cylindrical bending; in the exact solution these moments do no work because the generators

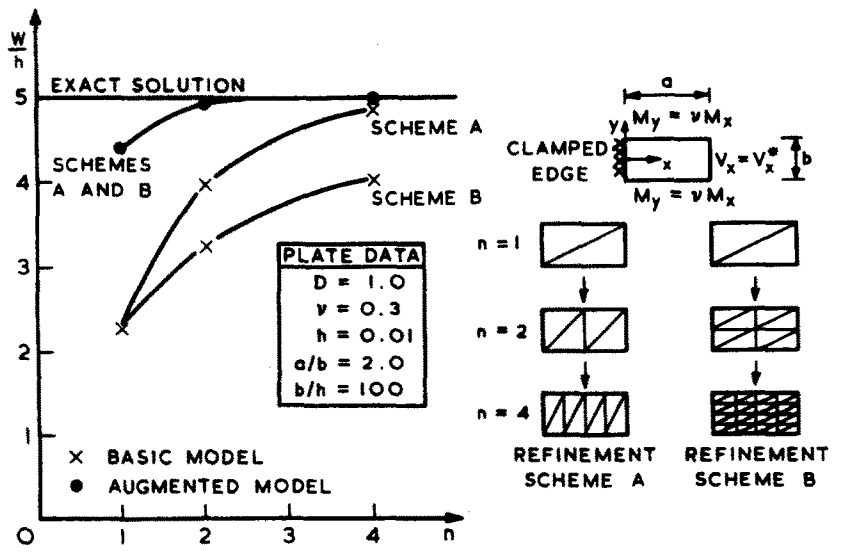

Fig. 1. Convergence study of tip deflections of rectangular cantilever plate using alternative mesh refinements.

are straight lines. The normal displacement of the mid-surface is given by

$$\frac{W}{h} = \frac{1}{6}\left(\frac{V_x^*}{Dh}\right)(3a - x)x^2, \tag{6-1}$$

where h is the thickness of the plate and

$$D = \frac{Eh^3}{12(1-\nu^2)} \tag{6-2}$$

is its flexural rigidity. The value of V_x^* is chosen to give a normal displacement $W/h = 5$ at the end $x = a$; this is the largest end-displacement which can be obtained using the basic finite element model before convergence problems affect the iterative solution. The augmented displacements model can attain much larger values of end-displacement without any difficulty with convergence.

The problem is analysed using two alternative schemes for refinement of the finite element mesh. Refinement scheme A increases the number of elements in the x-direction only. Refinement scheme B increases the number of elements in the x-direction and the y-direction simultaneously, i.e. a "consistent" refinement where the finest mesh includes the nodal points of all the coarser meshes. Scheme A has $2n$ elements for each level of mesh refinement, where n is the number of elements along the longitudinal edges $y = \pm b/2$, while scheme B has $2n^2$ elements. For the finest mesh, with $n = 4$, scheme A has eight elements and scheme B has thirty-two elements.

The results of the analyses are presented as a graph of end-displacement plotted against n. The augmented displacements model shows very rapid convergence to the exact solution with mesh refinement: the numerical solutions for schemes A and B are identical for any level of mesh refinement. By contrast, the basic finite element model shows slow convergence towards the exact solution and there is a marked difference between refinement schemes A and B. It is paradoxical that the latter scheme gives worse results with a much larger number of elements. Clearly, the basic finite element model is sensitive to the scheme of mesh refinement which is adopted and this is generally undesirable.

6.2 *Clamped square plate under central force*

This example concerns a thin square plate loaded by a concentrated normal force at the centre. The edges are rigidly clamped both against normal displacement and rotation and against membrane displacements. The latter boundary conditions restrict movement in the

plane of the plate and the applied loading tends to be resisted to an increasing extent by membrane forces which develop by stretching of the plate mid-surface.

At sufficiently high values of the applied load the behaviour of the plate is equivalent to that of a loaded membrane: in general there is a cubic relationship[2] between the central force and its corresponding normal displacement. The exact solution of a square membrane under a central force is unknown, but an analytic solution is available[18] for a circular membrane under a central force which is exact when Poisson's ratio $\nu = \frac{1}{3}$. In this case the normal displacement is given in terms of the central force P by

$$W = \left[\frac{3PR^2}{\pi Eh}\right]^{\frac{1}{3}}\left[1-\left(\frac{r}{R}\right)^{\frac{2}{3}}\right], \tag{6-3}$$

where r is the radial coordinate measured from the centre of a circular membrane of radius R. Equation (6-3) provides a fairly accurate representation of the load-displacement behaviour at the centre of a square plate of side length a if we put $R = a/2$. The appropriate relationship is

$$\frac{Pa^2}{Eh^4} = \frac{4\pi}{3}\left(\frac{W}{h}\right)^3_{r=0}, \tag{6-4}$$

which is plotted in Fig. 2.

A graph of central force against central displacement is shown in Fig. 2 for two sets of results obtained using the basic finite element model and the augmented displacements model respectively. Taking account of symmetry conditions, one-eighth of the plate is analysed using 16 elements. As anticipated, both sets of results lie on the same nonlinear curve because there is no inextensional bending action and hence the finite element idealizations are essentially the same. Now, the flexural rigidity of the plate has a significant influence on the behaviour at low values of the central force. The finite element models therefore predict an initially stiffer response than the circular membrane solution which neglects the flexural rigidity. But the results correctly show that the stiffness of the plate soon becomes identical to that of the circular membrane as the magnitude of the central force is increased. This is in marked contrast to the constant stiffness predicted by the small displacement theory.

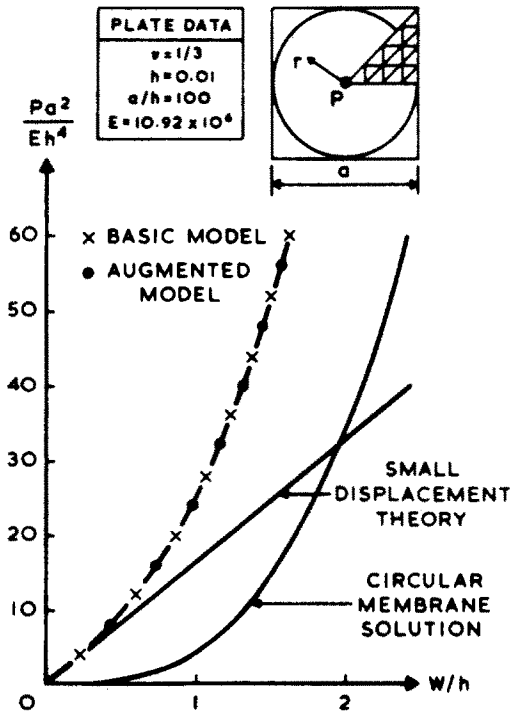

Fig. 2. Clamped square plate under central force

6.3 *Rhombic plate under corner forces*

This example is designed to investigate the effects of explicitly including simple inextensional bending deformations in the finite element trial functions of the augmented displacements model. The problem concerns the large displacement bending of a thin rhombic plate under the action of corner forces P, as shown in Fig. 3. The plate is supported by a rigid bar across its shorter diagonal, where the normal displacement is consequently zero, to eliminate any tendency to deform into an anticlastic surface at small values of the loading. This latter mode of deformation is associated with small displacement behaviour and it is irrelevant in the present context.

At large normal displacements the plate deforms into a cylinder with generators parallel to the shorter diagonal, apart from a narrow "boundary layer" close to each of the plate edges where there is a small deviation in normal displacement from the true cylinder. Here, the deformation is not inextensional: there is a membrane force in the boundary layer parallel to the plate edge and proportional to the deviations in normal displacement. However, a fairly accurate estimate of the normal displacements can be obtained from an analysis[11] which assumes that the deformation is entirely inextensional. In this case, the normal displacement of the mid-surface is a linear function of the applied load at a corner, viz:

$$\frac{W}{h} = \frac{Px^2}{4Dh} \cot \theta, \tag{6-5}$$

where h is the thickness of the plate, D is the flexural rigidity and θ is the half-angle between the concurrent edges at one of the corners of the plate (see Fig. 3).

Using conditions of symmetry, one quarter of the plate is analysed using a mesh of 16 elements both for the basic finite element model and for the augmented displacement model. The results are plotted in Fig. 3 as graphs of corner force against corner displacement. It is clear that the response calculated with the basic model is an unacceptable result: the plate is found to have an increasing resistance to the application of the corner forces. On the other hand, the linear response calculated with the augmented displacements model is a quite satisfactory solution which agrees with the prediction of inextensional theory.

6.4 *Rectangular plate under plane compression*

The final example is concerned with the finite element analysis of the elastic post-buckling behaviour of plates. The problem is to calculate the response of a thin simply-supported

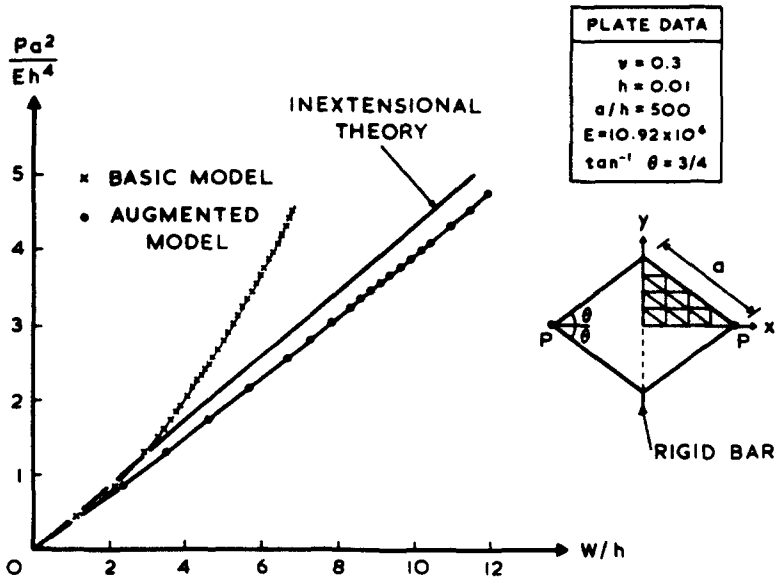

Fig. 3. Diagonally supported rhombic plate under corner forces.

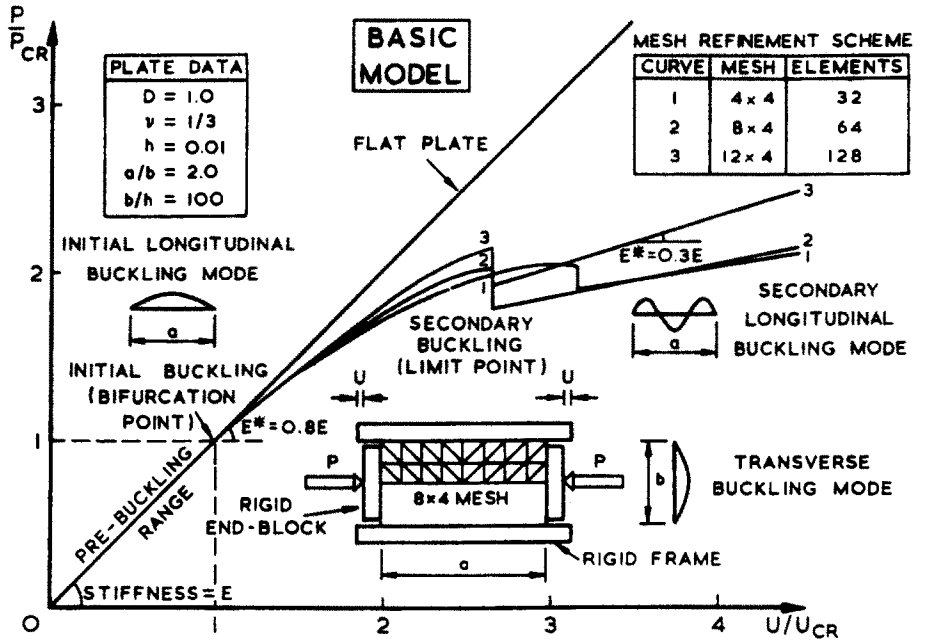

Fig. 4. Simply supported rectangular plate under plane compression.

rectangular plate under plane compression as shown in Figs. 4 and 5. The longitudinal edges of the plate are considered to be held in a rigid frame which completely restrains normal membrane displacements but freely permits the existence of tangential membrane displacements. Each transverse end of the plate is compressed by a force P applied through a rigid end-block, whose movement is denoted by the displacement U. In the pre-buckling range, the plate is assumed to remain flat and the force-displacement response is linear with constant stiffness E. At the initial buckling point the plate develops normal displacements, the mode shape having a single "buckle" in the longitudinal and transverse directions respectively. In the post-buckling range, the in-plane stiffness of the plate (denoted by E^*) decreases until secondary buckling occurs and the plate snaps into a new mode shape. In this case the mode is

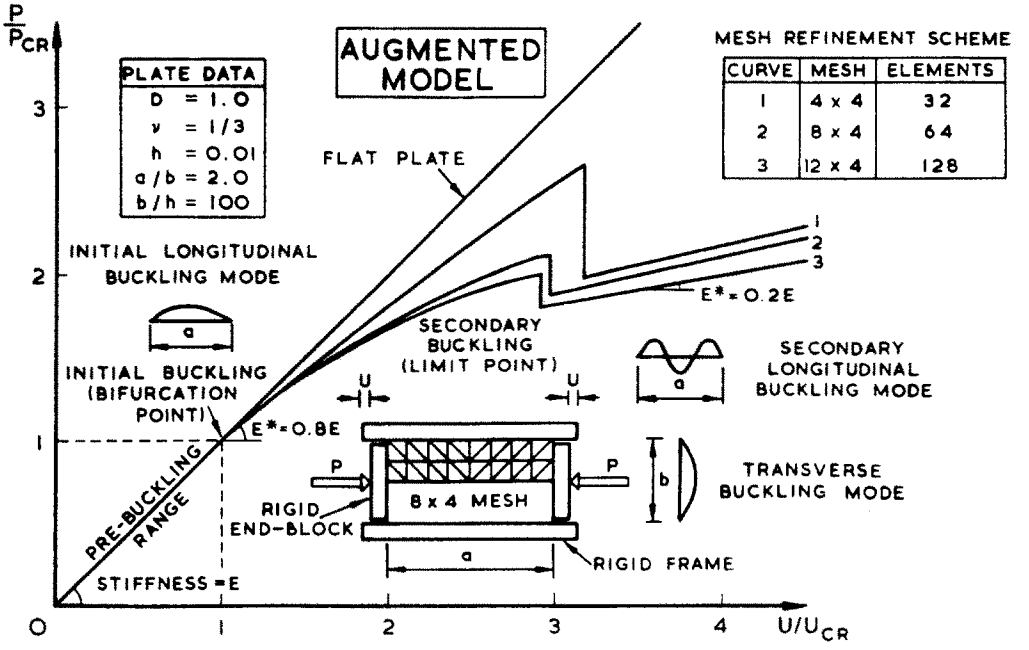

Fig. 5. Simply supported rectangular plate under plane compression.

found to have three buckles in the longitudinal direction. The maximum normal displacement is of the same order of magnitude as the plate thickness.

The finite element results for the basic model and the augmented displacements model are presented in Figs. 4 and 5 respectively. Half the plate is analysed, because of symmetry, using three finite element meshes with progressive refinement in the longitudinal direction only. The plate is compressed by increasing the end-displacement U; the associated force P is determined by integration of the longitudinal stress resultants at the end of the plate which are taken from the finite element analysis. The critical values P_{CR} and U_{CR} at the initial buckling point are calculated using the eigenvalue solution described in Ref. [9].

Curves of P/P_{CR} against U/U_{CR} are plotted in Fig. 4 for the basic finite element model. They show an obviously incorrect result where the calculated post-buckling response becomes stiffer with mesh refinement. It is also difficult to identify the position of the secondary buckling point because of the irregular pattern of the curves in this region. By contrast, the corresponding force-displacement curves for the augmented displacements model plotted in Fig. 5 provide a more credible numerical solution. Here, the post-buckling response is found to become less stiff with mesh refinement, as usually expected from this type of finite element analysis. Moreover, clear evidence of smooth convergence characteristics is provided by the regular sequence of curves in the region of the secondary buckling point. It is a noteworthy practical demonstration of the beneficial effect of including simple inextensional bending actions in the finite element trial functions.

7. CONCLUSIONS

The present paper is concerned with the development of finite element models for accurate analysis of the class of plate problems covered by the nonlinear theory of von Kármán. In this context, triangular finite elements are presented for the large displacement bending and post-buckling analysis of thin plates. The formulation is based upon a general variational theory for large displacement bending which is free from restrictive subsidiary conditions on the stress and displacement variables. This offers a wide scope for the selection of finite element trial functions to model the particular physical actions identified as crucial to the successful calculation of large displacement behaviour. Indeed, it is shown that basic trial functions can be easily adapted to allow exact recovery of the important inextensional bending deformations in addition to rigid body movements and constant states of membrane strain. Further developments to deal with more complicated types of physical action, such as boundary layer effects, are also feasible using this type of approach.

The paper presents a selection of numerical examples which include various kinds of elastic behaviour typical of the large displacement bending and post-buckling of thin plates. It is found that a notable improvement in performance is achieved using a finite element model with simple inextensional bending deformations included in the trial functions. Yet there is no significant increase in the computational effort required for a numerical solution when this feature is incorporated in the analysis. In all cases where the effect of refining the finite element mesh is investigated, the results obtained with this type of finite element model exhibit rapid and smooth convergence to the final solution. This provides a first validation of the fundamental requirements proposed for accurate finite element analysis of nonlinear elastic plate bending.

REFERENCES

1. S. Timoshenko and S. Woinowsky-Krieger, *Theory of Plates and Shells*. 2nd Edn McGraw-Hill, New York (1959).
2. E. H. Mansfield, *The Bending and Stretching of Plates*. Pergamon Press, Oxford (1964).
3. T. von Kármán, *Enclopädie der Mathematischen Wissenschaften*. Vol. 4, p. 349 B. G. Teubner, Leipzig (1910).
4. T. H. H. Pian, Derivation of element stiffness matrices by assumed stress distributions. *AIAA J.* **2**, p. 1333–1336 (1964).
5. T. H. H. Pian, Element stiffness matrices for boundary compatibility and for prescribed boundary stresses. *Proc. 1st Conf. on Matrix Methods in Structural Mechanics*, AFFDL-TR-66-80, pp. 457–477, Nov. 1966.
6. D. J. Allman, Triangular finite elements for plate bending with constant and linearly varying bending moments. *Proc. IUTAM Symp. on High Speed Computing of Elastic Structures*, University of Liège, pp. 105–136 (1971).
7. B. Tabarrok and N. Gass, A variational formulation for plate buckling problems by the hybrid finite element method. *Int. J. Solids Structures* **14**, pp. 67–80 (1978).
8. D. J. Allman, Finite element analysis of plate buckling using a mixed variational principle. *Proc. 3rd Conf. on Matrix Methods in Structural Mechanics*, AFFDL-TR-71-60, pp. 683–705, December 1973.
9. D. J. Allman, Calculation of the elastic buckling loads of thin flat reinforced plates using triangular finite elements. *Int. J. Num. Meth. Engng* **9**, pp. 415–432 (1975).

10. P. L. Boland and T. H. H. Pian, Large deflection analysis of thin elastic structures by the assumed stress finite element method. *Computers and Structures* 7, pp. 1–12 (1977).
11. D. J. Allman, Variational theory for large displacement bending of thin plates. *RAE Tech. Rep.* 80108 (1980).
12. D. J. Allman, Some fundamental aspects of the finite element analysis of nonlinear elastic plate bending. *RAE Tech. Rep.* 80090 (1980).
13. G. Strang and G. J. Fix, *An Analysis of the Finite Element Method.* Prentice-Hall, Englewood Cliffs, New Jersey (1973).
14. G. P. Bazeley, Y. K. Cheung, B. M. Irons and O. C. Zienkiewicz, Triangular elements in plate bending—conforming and non-conforming solutions. *Proc. 1st Conf. on Matrix Methods in Structural Mechanics*, AFFDL-TR-66-80, pp. 547–576 (1966).
15. D. J. Allman, A simple cubic displacement element for plate bending. *Int. J. Num. Meth. Engng* **10**, pp. 263–281 (1976).
16. P. Bartholomew, Comment on hybrid finite elements. *Int. J. Num. Meth. Engng* **10**, pp. 968–973 (1976).
17. D. J. Allman, On compatible and equilibrium models with linear stresses for stretching of elastic plates. *Energy Methods in Finite Element Analysis* (Edited by R. Glowinski, E. Y. Rodin and O. C. Zienkiewicz), pp. 111–126. Wiley, New York (1979).
18. D. J. Allman and E. H. Mansfield, The annular membrane under axial load. *RAE Tech. Memo. Structures* 978 (1981).
19. B. Tabarrok and S. Dost, Some variational formulations for large deformation analysis of plates. *J. Comput. Meth. Appl. Mech. Engng* **22**, pp. 279–288 (1980).